

Observing higher modes of gravitational radiation in future detectors

Divyajyoti^{1,2}, Preet Baxi^{1,2}, Chandra Kant Mishra^{1,2}, K. G. Arun³

¹Indian Institute of Technology Madras

²Center for Strings, Gravitation and Cosmology, IIT Madras

³Chennai Mathematical Institute

Phys. Rev. D 104, 084080, arXiv: 2103.03241

divyajyoti@physics.iitm.ac.in

Chennai Symposium on Gravitation and Cosmology (CSGC)

February 3, 2022

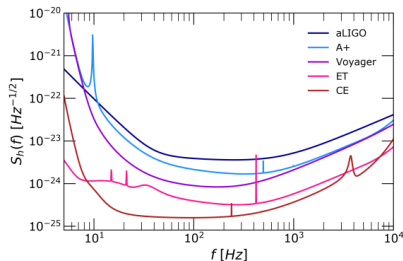


Introduction

- In GWTC-2, LIGO-Virgo Collaboration reported the detection of Higher Modes (HMs) for two events: GW190412 and GW190814.
- A few more events with large mass ratios have been added in GWTC-3.
- Relative contribution of HMs increases for binary systems which are asymmetric in masses, or non-optimally oriented.
- Detection of HMs increases the mass reach of the detectors, leads to better parameter estimation and measurement of cosmological parameters.
- We have performed three studies:
 - Detectability of HMs in $q - \iota$ plane
 - Detection of HMs for GWTC-2 events if 3G detectors were operational
 - Population study using the next generation detector networks.

Detector networks

- Upgraded 2G detectors: LIGO-A+, Voyager
- 3G detectors:
 - Cosmic Explorer (CE): L-shaped, length of each arm = 40km.
 - Einstein telescope (ET): Equilateral triangle, length of each arm = 10km, setup will be underground.
 - Low frequency sensitivity in the range of 1-5Hz.



Label	Location	Type(s)
L	Louisiana, USA	CE/A+/Voyager
H	Washington, USA	CE/A+/Voyager
V	Cascina, Italy	CE/A+/Voyager
A	New South Wales, Australia	CE
E	Cascina, Italy	ET

Waveform and detection criteria

- Multipolar expansion of GW radiation:

$$h(t; \iota, \varphi_o) = \frac{1}{d_L} \sum_{\ell=2}^{\infty} \sum_{m=-\ell}^{\ell} h_{\ell m}(t, \lambda) Y_{\ell m}^{-2}(\iota, \varphi_o) \quad (1)$$

- Waveform: IMRPhenomHM, Modes (ℓ, m) : 22, 33, 44, 21, 32, 43.
- Individual mode strain:

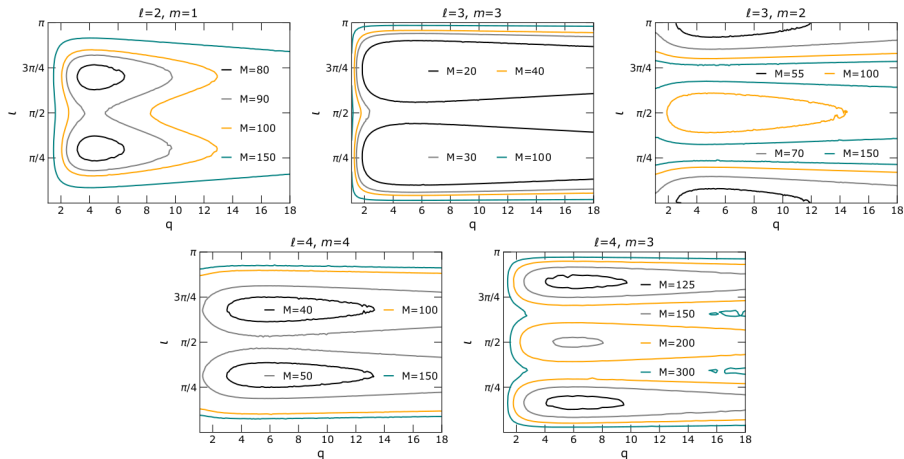
$$\tilde{h}_{\ell m}(f) = F_+(\theta, \phi, \psi) \tilde{h}_+^{\ell m}(f) + F_\times(\theta, \phi, \psi) \tilde{h}_\times^{\ell m}(f) \quad (2)$$

- Optimal SNR for each mode $(\rho_{\ell m})$ as:

$$\rho_{\ell m}^2 = 4 \int_{f_{\text{low}}}^{f_{\text{cut}}} \frac{|\tilde{h}_{\ell m}(f)|^2}{S_h(f)} df \quad (3)$$

- $f_{\text{low}} = 5\text{Hz}$ for all the detectors.
- Criteria for detection: 22 mode: $\text{SNR} \geq 10$, HMs: $\text{SNR} \geq 3$

Higher modes in the $q - \iota$ plane



Fixed SNR=3, $D_L = 3$ Gpc, $\chi_{1z} = 0.9$, $\chi_{2z} = 0.8$, Detector: CE

HM SNRs in CE for GWTC-2 events

Event	M	q	χ_{eff}	SNR in mode				
				22	33	44	21	32
GW190412	42.6	3.2	0.2	649	81	17	14	3.9
GW190519_153544	159.5	1.6	0.4	685	79	48	19	14
GW190521	279.8	1.4	0.1	424	22	19	7.1	7.5
GW190602_175927	173.8	1.4	0.1	330	15	9.4	4.3	4.7
GW190630_185205	69.9	1.5	0.1	708	31	14	7.9	5.8
GW190706_222641	183.5	1.7	0.3	223	18	7.6	3.4	3.3
GW190814	27.2	9.0	0	982	172	33	32	4.4
GW190828_065509	44.4	2.4	0.1	418	34	7.2	6.7	3.0

LIGO-Virgo quoted the 33 mode network SNR as ~ 6.6 for GW190814.

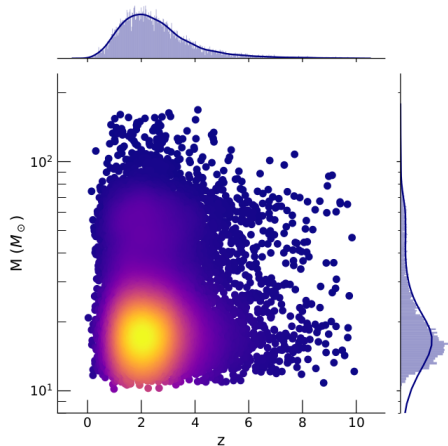
Population Study: Models

- Models (from GWTC-2¹) for the parameter distributions chosen as:
 - Masses: POWER LAW + PEAK and BROKEN POWER LAW models.
 $m_1 \in (5, 100)$, $q_{\max} = 18$.
 - Spins: DEFAULT MODEL for both χ_{1z} and χ_{2z} , range $\{-1,1\}$.
 - Luminosity Distance: Madau-Dickinson redshift evolution model²,
 $z_{\max} = 10$.
 - Angles: $\cos(\iota)$ and $\cos(\theta)$ uniform between $\{-1,1\}$, ϕ and ψ uniform between $\{0,\pi\}$.
- Total number of population points for each mode: 10,000

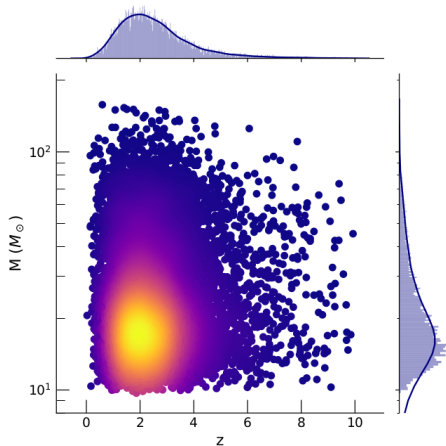
¹R. Abbott et al. (LIGO Scientific, Virgo) (2020), arXiv:2010.14533.

²K. K. Y. Ng et al., Astrophys. J. Lett. 913, L5 (2021), arXiv:2012.09876.

Injected Population

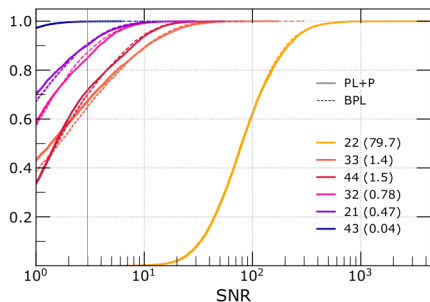


POWER LAW + PEAK (PLP)



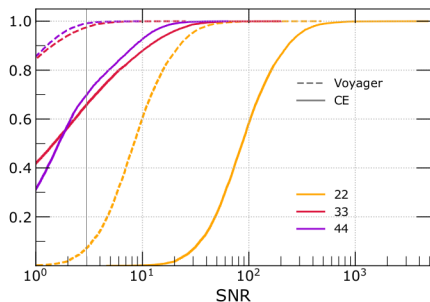
BROKEN POWER LAW (BPL)

Population histograms



Comparison between mass models
(PL+P and BPL)

3G Detector network: LAE



Comparison between generations
of detectors

Detector network: LHV for both
the detectors (Voyager, CE)

Results and Summary

- Different HMs activate different regions of the parameter space, and show symmetries in ι leading to bi- and tri- modality of contours.
- Several of the GWTC-2 events would've led to the detection of HMs if 3G detectors were operational now.
- For 3G network, 33 and 44 modes are detectable in nearly 30% of the population.
- For 10% of the sources, all five leading modes are detectable.
- Comparison between generations: Less than 10% sources show detectability of 33 and 44 modes for upgraded 2G detectors, whereas for 3G, this number is $\sim 30\%$.

Thank You

- Plus and cross polarizations associated with each mode:

$$\begin{aligned}\tilde{h}_+^{\ell m}(f) &= \left[(-)^{\ell} \frac{d_2^{\ell, -m}(\iota)}{d_2^{\ell m}(\iota)} + 1 \right] Y_{-2}^{\ell m}(\iota, \varphi_0) \tilde{h}_{\ell m}^{\text{R}}(f) \\ \tilde{h}_{\times}^{\ell m}(f) &= -i \left[(-)^{\ell} \frac{d_2^{\ell, -m}(\iota)}{d_2^{\ell m}(\iota)} - 1 \right] Y_{-2}^{\ell m}(\iota, \varphi_0) \tilde{h}_{\ell m}^{\text{R}}(f)\end{aligned}\tag{4}$$

where $\tilde{h}_{\ell m}^{\text{R}}(f) = A_{\ell m}(f) e^{i\varphi_{\ell m}(f)}$

- Combining them with the detector pattern functions:

$$\tilde{h}_{\ell m}(f) = F_+(\theta, \phi, \psi) \tilde{h}_+^{\ell m}(f) + F_{\times}(\theta, \phi, \psi) \tilde{h}_{\times}^{\ell m}(f)\tag{5}$$